DOI:10.53539/squjs.vol29iss1pp68-85

Sultan Qaboos University Journal for Science

Journal page: www.squ.edu.om/index.php/squjs/index

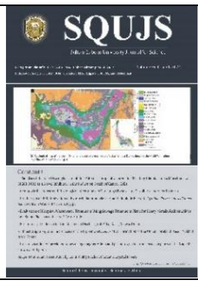

Lithostratigraphy and Microfacies of the Upper Cretaceous Muti Formation of the Oman Foreland Basin, Nakhal Area, Oman

Jenan Ahmed Attar[1], Iftikhar Ahmed Abbasi[1*], Muhammad Hanif[4], Mohamed A.K. El-Ghali[1,2], Abdulrazaq Al-Sayigh[1], Abdul Rahman Al-Harthi[3]

[1]Department of Earth Sciences, College of Sciences, Sultan Qaboos University, Muscat, Sultanate of Oman, [2]Earth Sciences Research Center, Sultan Qaboos University, Muscat, Sultanate of Oman, [3]Exploration Department, PDO, Muscat, Sultanate of Oman, [4]National Centre of Excellence in Geology, University of Peshawar, Pakistan.

*Corresponding author email address: iftikhar@squ.edu.om

ARTICLE HISTORY

Received 29 May 2023
Received revised 17 October 2023
Accepted 23 October 2023

ABSTRACT

The Upper Cretaceous Muti Formation was deposited in the Oman Foreland Basin during the obduction of the allochthonous units on the eastern margin of the Arabian Platform. The formation is exposed in various isolated outcrops around Jabal Akhdar Mountain and is located between the Mesozoic platform carbonates below and the allochthonous nappe above. The current study is the first to describe the outcrops of the Muti Formation in the Nakhal area. It focuses on the lithofacies, microfacies distribution, and the characterization of the depositional environment of the formation. The lithofacies and microfacies of the formation are described from two measured sections in the study area. The Nakhal section is about 50 m thick and consists of four lithofacies: marl, bedded limestone, nodular limestone, and clay. A total of four microfacies are identified, including echinoderm-spine wackestone, bioclastic packestone, arenaceous wackestone, and mudstone. Diagenetic features such as fractures, cementations, and dissolutions, and their products, for instance, porosities, were also identified, and their paragenetic history was reconstructed. Additionally, microfossils, such as bryozoan fragments, calcispheres, bivalves, fragments of echinoids, and brachiopod fragments, benthic and planktonic foraminifera were recognized. Based on lithological and biotic variations, it is suggested that the Muti Formation in the Nakhal area was deposited in a shallow marine environment on the outer to the mid-carbonate shelves. This formation is subjected to diagenetic changes starting with eogenesis in marine settings followed by burial diagenesis, and subsequently, the formation is exposed to the telogenetic diagenesis phase.

Keywords: Muti Formation, Nakhal Area, Oman Foreland Basin, Upper Cretaceous, Jabal Akhdar.

توزيع الصخور الجيولوجية و السحنات الدقيقة لاواخر العصر الطباشيري لتكوين موطي في حوض فورلاند عمان ، منطقة نخل، سلطنة عمان

جنان أحمد عطار[1]، افتخار أحمد عباسي[1*]، محمد حنيف[4]، محمد الغالي[1،2]، عبدالرزاق الصايغ[1]، عبدالرحمن الحارثي[3]

الملخص: تم ترسيب تكوين موطي في أواخر العصر الطباشيري في حوض الفورلاند خلال اندفاع الوحدات الغير منسوبة إلى مكانها الأصلي على الجانب الشرقي للصفيحة العربية. تكوين موطي ينتشر في نتوءات منفصلة حول الجبل الأخضر ويقع بين صفيحة الكربونات للعصر الوسيط في الأسفل و الوحدات الغير منسوبة إلى مكانها الأصلي في الأعلى. هذة الدراسة تعتبرالدراسة الأولى لنتوءات تكوين موطي في منطقة نخل. يتم بها وصف توزيع الصخور الجيولوجية، السحنات الدقيقة، ووصف البيئة الترسبية للتكوين. الصخور الجيولوجية و السحنات الدقيقة للتكوين تمت دراستها في مقطعين مقاسين للتكوين في المنطقة الدراسية. سمك مقطع نخل حوالي 50 مترا ويتألف من أربعة أنواع من الصخور الجيولوجية: التراب الكلسي، طبقات الحجر الجيري، الحجر الجيري المجور، والطين. كما تم

تحديد التحورات المميزة مثل: الشقوق، التدعيمات الكربونية، الانحلالات، ونتائجها مثل: الفجوات وتم بناء تاريخ التحورات. بالإضافة إلى ذلك، تم التعرف على الكائنات الحية الدقيقة مثل: قطع من البريزون، والكالسيسفير، وقشريات بحرية، و قطع من البراكيوبود، و قطع من الرخويات، و نوعين من فورامنيفر العوالق والقاعية. استنادا إلى التباينات الصخرية والبيولوجية، يقترح أن تكوين الموطي في منطقة نخل تم ترسيبة في بيئة بحرية ضحلة على الرفوف الكربونية الخارجية إلى المتوسطة. هذا التكوين تعرض للتحورات تبدأ من التكوين (ايوجينسيس) في البيئة البحرية، تليها التحور خلال الدفن (بيريال) ، وبعد ذلك تعرض للتحور عند التيلوجينيسيس.

الكلمات المفتاحية: تكوين موطي، منطقة نخل، حوض عمان الفورلاند، أواخر العصر الطباشيري، الجبل الأخضر.

1. Introduction

This publication delves into a comprehensive study of the Muti Formation, deposited during the early stages of the Oman Foreland Basin's development, which emerged as a consequence of the obduction of the Semail Ophiolite and Hawasina nappe onto the existing carbonate platform [1,2,3,4,5 and numerous references therein]. The establishment of the foreland basin marked the cessation of carbonate production in the Hajar Supergroup, possibly due to drowning, followed by the introduction of siliciclastic sediments in certain basin regions, including the Nakhal area [1,3]. An intricate analysis of the Muti Formation offers valuable insights into the dynamic processes that characterized the basin's initial phases, as these sediments were laid down once carbonate production ceased on the platform.

The Muti Formation, constituting the lower part of the Upper Cretaceous Aruma Group, comprises a diverse range of lithologies, including carbonaceous siltstone, limestone, mudstone, and conglomerate, distributed across various sectors of the foreland basin. The Aruma Group is well exposed at a number of localities in the Jabal Al Akhdar and Al Hajar Mountains, whereas it is wedging out towards the Al Huqf-Haima High axis in the south and east directions [6, 7]. The Muti Formation is laterally equivalent to the Fiqa Formation in the subsurface of the Oman sedimentary basins [1].

This study centers on a well-exposed section of the Muti Formation located in the Nakhal area, situated in the northern region of the Jabal-Akhdar Dome (Figure 1a) [8]. Based on its lithological attributes, the Muti Formation is subdivided into the Sayga and Riyamah members [1, 3]. In the Nakhal area (Figure 1b), the Sayga Member of the Muti Formation enjoys prominent exposure, and the primary focus of this investigation revolves around elucidating its lithostratigraphy and microfacies in order to gain insights into its depositional environment. Throughout this paper, we shall refer to the Sayga member when mentioning the Muti Formation, as the Riyamah member remains unobservable in the Nakhal area.

2. Regional Geology

The Muti Formation was deposited in the Oman Foreland Basin during the Late Cretaceous and is exposed around Jabal Akhdar, Saih Hitat, and Jabal Salakh mountains [1, 3]. The Oman Mountains were developed during the Late Cretaceous to Miocene through the first and second Alpine events [9]. The first Alpine event is marked by the obduction and thrusting of the allochthonous units, Semail Ophiolite and Hawasina Nappe, over the carbonate platform, in the northeast portion of the Arabian Plate. The Atlantic Ocean started to open during this period, and the Arabian-African plate drifted northward [4]. This event, combined with the opposite rotation of Eurasia and Africa, initiated the closure of the Neo-Tethys, and the intra-oceanic convergence began in the Neotethys northeast of the Oman passive margin [5]. At the early stages of the closure of the Neo-Tethys ocean, downwarping of the Arabian continental margin, combined with the compressional forces of closure from the Eurasian plate, initiated obduction of the Tethyan oceanic crust along preexisting transform faults and the hot oceanic crust was detached along oblique NE dipping thrust faults [4]. Consequently, the loading of the allochthonous units led the northeast portion of the Arabian platform to bend and flex, and a foreland basin developed in the depression between the obducted allochthon and an emergent peripheral bulge to the west [2, 10, 11]. In the second Alpine event, the Arabian plate collided with the Eurasian plate in the Zagros region. This resulted in the significant culmination of the Oman Mountains in the front of the fold and thrust belt and adjacent to the Oman Foreland Basin (Figure 2) [9, 12] .

During the early Turonian, the top of the carbonate platform sediments of the Natih Formation were truncated toward the northeast direction, associated with developing a regional hard ground [9, 12, 13, 14]. This contact is known as Wasia- Aruma break and it extends from the northeast portion of Oman toward the eastern part of the UAE [13]. The period of the formation of this contact is linked with the initial stage of collision between the Arabian margin and the Tethyan subduction zone and the formation of the forebulge [12]. In some areas around Jabal-Akhdar Dome, the hardground contact represents the top of the Kahmah Group (Figure 3). This shows that the erosion at the end of Cenomaian was synchronous with the upwarping of the northern part of Jabal Akhdar [15].

3. Stratigraphy

The Oman Foreland Basin was filled with sediments that were derived primarily from the adjacent thrust and fold belt [7]. These sediments, representing the Aruma Group and

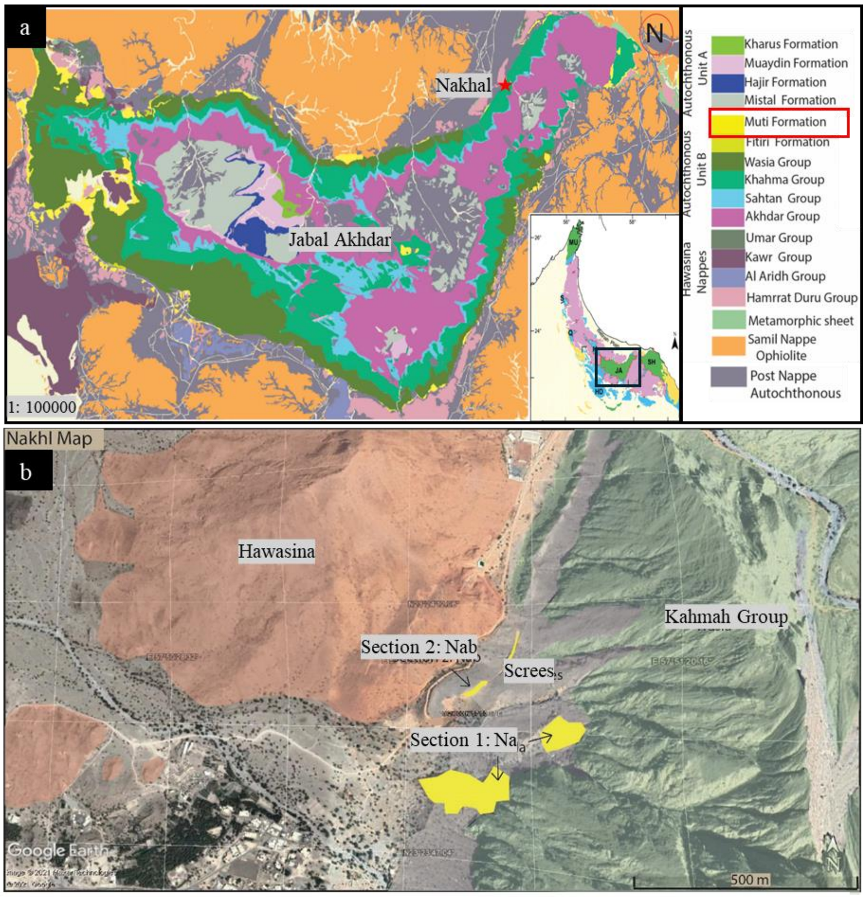

Figure 1. (a) Geological map of northern Oman and detailed sketch map of Jabal-Akhdar Dome showing the Muti Formation in yellow color [8] and (b) sketch map of Nakhal area showing the locations of studied outcrops Section 1: Na and Section 2: Nab.

were deposited during the Upper Cretaceous (Figure 4) [3]. The Aruma Group consists of Muti, Juweiza, Simsima and Qahlah formations in the Oman Mountains, whereas most of the Fiqa Formation is present in subsurface in Oman Sedimentary basins [3]. The Muti Formation was deposited in the foreland basin during the early stage of basin development, is divided into two members; Sayga and Riyamah [3]. The Sayga member is exposed around Jabal Akhdar, Saih Hatat, and Jabal Salakh (Figure 2)[1], and is focus of the present study in Nakhal area (Figure 1b).

In Nakhal area, the Muti Formation unconformably overlies the Kahmah Group [15], however, in other areas around Jabal-Akhdar Dome, it unconformably overlies the Wasia Group [3, 6, 13, 15], indicating that the Wasia Group has been completely eroded in this area prior to the deposition of the Muti Formation. The top surface of the Kahmah Group was subjected to the same conditions as the Wasia Group; the hardground surface represented the drained surface for a long time without sedimentation before the Muti Formation sediments started to deposit (Figure 3).

The Sayga member of the Muti Formation is subdivided into an upper and lower part. The lower section is composed of concretionary and bioclastic argillaceous limestones that are rich in echinoids, bryozoans, bivalves, shell fragments, micritic intraclasts, and ooids. In contrast, the upper part is made of mudstone and calcareous shales, and occasionally contains quartzose siltstone and sandstone. The calcareous shales contain shallow benthic biomicrite and pelagic microfossils.

4. Study area

The town of Nakhal is situated in the Batinah region, to the north of the Jabal-Akhdar Dome, at a distance of approximately 100 kilometers from Muscat (Figure 1). Two distinct sections, namely Nakhal Na and Nakhal Nab, were identified and investigated within the Nakhal area (Figure 2b). The Na Section, was both measured and sampled, while Nab Section was only sampled. The coordinates of Section Na are 23° 23' 53.65" N and 57° 51' 1.25" E, locates at a ridge face with an elevation of around 300 meters above the road. On the other hand, section Nab, located approximately 200 meters north of Section Na, is situated at coordinates 23° 24' 02.03" N and 57° 51' 03.22" E (Figure 1b).

5. Materials and Methodology

Two sections were measured and described in the Nakhal area for sedimentological analysis (Figure 5). Section Na has been thoroughly logged, sampled and described, while Section Nab was only sampled due to the difficulties in identifying the upper and lower contacts. The

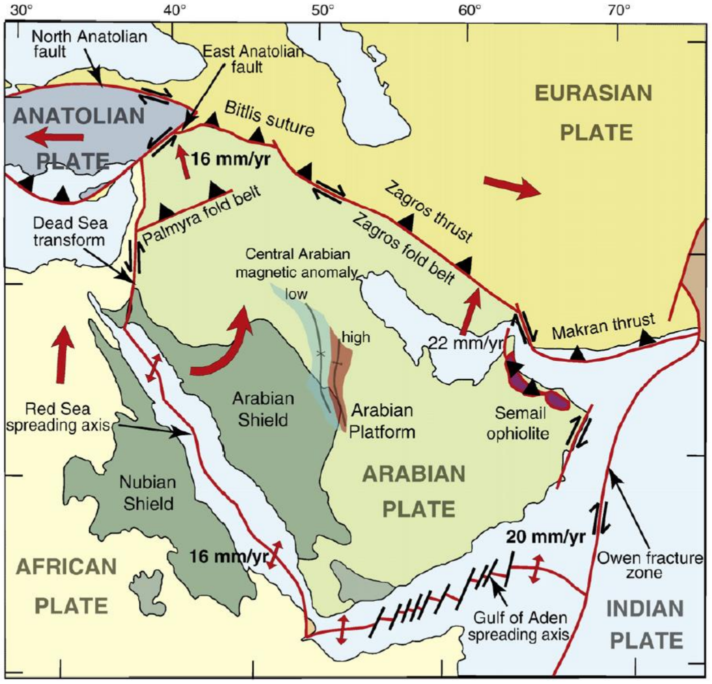

Figure 2. Location map of the Arabian Plate showing different plate tectonic settings and elements around Oman. Modified after [16]

Figure 3. Field photographs of a hardground surface shows the iron nodules, scale: pen 13.5 cm and person height around 1.75 m.

lithofacies types are classified based on grain size, clasts type, sedimentary structure, texture, and fossil content. A total of 18 rock samples were collected from the study area.

Seven selected samples were subjected to the standard thin section for petrographic analysis using a light transmission microscope. A few thin sections were half stained with Alizarin Red S and Potassium Ferricyanide following Dickson's methodology [17] for dolomite identification. The microfacies are named based on Dunham's classification [18] and their representative features.

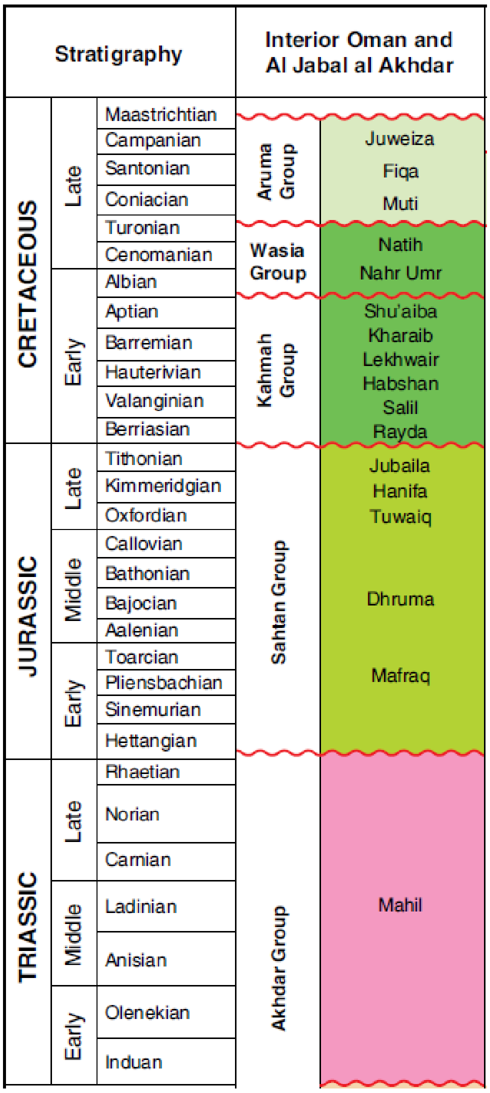

Figure 4. Stratigraphic column of interior Oman and Jabal Akhdar [19].

6. Results

6.1. Lithofacies

The studied Section Na is about 50 m thick in the Nakhal area and comprises four main lithofacies; marl, bedded limestone, nodular limestone, and clay. The cumulative thicknesses of these lithofacies are 6 m, 23.7 m, 6.5 m, and 2 m, respectively (Figures 5,6a). The lowermost 10 m of the logged section is covered with scree, which is thought to be composed mainly of marl. The overlying unit consists of marl and bedded limestone, which are followed by bedded limestone, and nodular limestone.

The clay lithofacies in the section are red and buff in color. Most of the limestone is interbedded with buff-colored clay, while red clay is found in compacted strips within limestone in the upper portion of the logged section. On the other hand, Section Nab, which is located approximately 200 m north of Section Na, is mostly buried under the scree. Consequently, only one lithofacies, the nodular limestone, was observed and sampled from this section (Figure 7b). The thickness of this unit ranges from 10 to 12 meters and is highly compacted. The nodular limestone is interbedded with reddish-to-brown clay. A detailed description of each lithofacies is provided below.

6.1.1. Marl (Ma)

Marl lithofacies is abundantly distributed in the lower part of the Muti Formation in Nakhal Section Na (Figure 6). The Ma lithofacies buff in color. It is laminated to thin-bedded, individual beds range from 0.5 cm to 1.5 cm. At places, the Ma lithofacies is interbedded with buff-colored clay and also contained patches of red clay (Figure 7a). The lithofacies Ma is moderately to well compacted. Angular to subangular white color carbonate clasts (millimeters in size) were observed in this lithofacies at the base of the section (Figures 5,7b). Fossil fragments and subangular to subrounded black color carbonate clasts were observed (Figure 7a).

Interpretation: Marl is a fine-grained arenaceous carbonate rock, chemically or biochemically precipitated from seawater [20]. Marl is deposited in a quiet water area with minor amount of siliciclastic input under low energy conditions [20, 21]. The water depth for the quiet-water deposition is impossible to determine because it can be both shallow and deep [23].

6.1.2. Bedded Limestone (BL)

The bedded limestone lithofacies (BL) is compacted, buff, red, and grey in color (Figures 5, 7c). The colors vary within the same bed. Commonly, the upper part of the section is more reddish in color. The lithofacies is laminated to thinly bedded. The total thickness of bedded limestone lithofacies is around 23 m. The average thickness of a single bed is about 3.5 cm. Most of the BL lithofacies are interbedded with buff color clay lithofacies. Red clay strips of less than 1 cm thick are interbedded with BL lithofacies in the upper part of the logged section Na (Figure 7c). In addition, iron concretions and calcite veins are also observed in the lithofacies.

Interpretation: The bedded limestone lithofacies was deposited in moderate energy in warm water settings [22]. The different colors of carbonate rocks are due to various factors, such as the input of detrital material and the post-sedimentary diagenetic processes [20]. The bedding and lamination are usually caused by slight differences in the physical circumstances, such as sediment supply and water flow [24].

6.1.3. Nodular Limestone (NL)

The nodular limestone lithofacies constitute the majority of the exposed section of Nab and the uppermost part of the Na Section (Figures 5, 7d-f). It is about 10 m thick in Nab Section and around 6 m in Na Section. The lithofacies consists of grey-colored carbonate nodules surrounded by buff-colored fine grains of carbonate matrix. The nodules sizes range between 4 cm to 20 cm in diameter, elongated, subrounded to subangular shapes. The boundaries between the nodules and the surrounding matrix are distinct. The limestone nodules laterally join each other. These lithofacies are highly compacted and contains an oxidation surface.

Interpretation: The nodular fabric forms in various depositional settings ranging from shallow to deep marine [20]. Generally, three main processes can develop this fabric: diagenetic, bioturbation and tectonics [20, 25, 26]. In the studied sections, most nodules are oriented parallel to the bed, have smooth contact, and lack grading. All these features indicate that it formed due to in situ processes such as differential compaction due to thin clay interbeds in limestone sequences. It may also be due to diagenetic processes with different rates of sedimentation and compaction from one place to another [26, 27].

6.1.4 Clay (Cl)

Clay lithofacies are found throughout the logged section and are interbedded with bedded limestone and other lithofacies (Figure 6). The Cl lithofacies thicknesses range from 1 cm to 3 cm. It is buff and red in color. The buff color clays are soft, whereas the red clays are compacted, forming less than 1 cm thick strips (Figures 7c, d).

Interpretation: The clay minerals are mainly of extrabasinal origin. They release as particles from the parent rocks during weathering and are transported long distances to the depositional basin and deposited out of suspension in quiet water conditions [20].

6.2. Microfacies

In the Nakhal section, a detailed study of the Muti Formation was conducted using seven standard thin sections. From this analysis, four distinct microfacies were identified: namely echinoderm spines wackestone, bioclastic packestone, arenaceous wackestone, and mudstone. The microfacies were classified based on distinguishing characteristics, such as texture, fossils and color. The thin sections were half-stained with Alizarin Red S and Potassium Ferricyanide for mineral identification following Dickson's methodology (Figure 9) [17]. The main objective of staining was to ascertain the composition of the cement, specifically whether it comprised calcite or dolomite, and to detect the presence of iron. The staining process revealed that all the examined thin sections exclusively contained calcite and were notably abundant in iron oxide. The following sections provide detailed descriptions and interpretations of the recognized microfacies. Table 1 provides a comprehensive summary of the framework composition of each microfacies.

Table 1. A summary table of the framework composition of each microfacies in Nakhal area, (tr-traces).

MF	Matrix (micrite) (%)	Skeletal grains (%)	Non-skeletal grains					Calcite cement (%)	Authigenic iron (%)
			Peloids (%)	Detrital iron (%)	Detrital quartz (%)	Zircon	Mica (%)		
MF1	47	3	-	15	19	tr	-	3	13
MF2	40	19	0.5	8	25	-	0.5	-	7
MF3	65	5	1	5	20	tr	-	-	4
MF4	80	1	2	1	4	tr	-	8	4

6.2.1. Microfacies 1: Echinoderm Spines Wackestone (MF1; ESW)

Echinoderm spines wackestone microfacies is observed in the lower part of the Nakhal section (Na) represented by two samples, Na3 and Na4 (Figure 9; Table 1). This microfacies is densely packed and characterized by longitudinal sections of echinoderm spines measuring between 1.1 mm and 1.3 mm in length (Figure 9a), comprising about 3% of the overall composition of the thin section. The spine is made up of a single calcite crystal with unit extinction [28].

The matrix of this microfacies primarily comprises carbonate mud micrite, accounting for 47% of the overall thin section components. Remarkably, around 28% of the matrix comprises detrital and authigenic iron (Figure 9b). Moreover, iron-filled burrows were observed (Figure 9c). The dominant grains in this microfacies are detrital quartz, ranging in size from coarse silt to very fine sand (Figures 10a,b). The percentage of quartz as a part of framework components based on Terry and Chilingar classification [29] is about 19%. Furthermore, rare zircon grains were observed.

Diagenesis

The main diagenetic features identified are fractures filled by cement and dissolution. Some of these features represent multiple diagenetic generations. A few fractures run across the thin-section, filled with carbonate cement and rare quartz (Figure 9d). Other types of fractures include

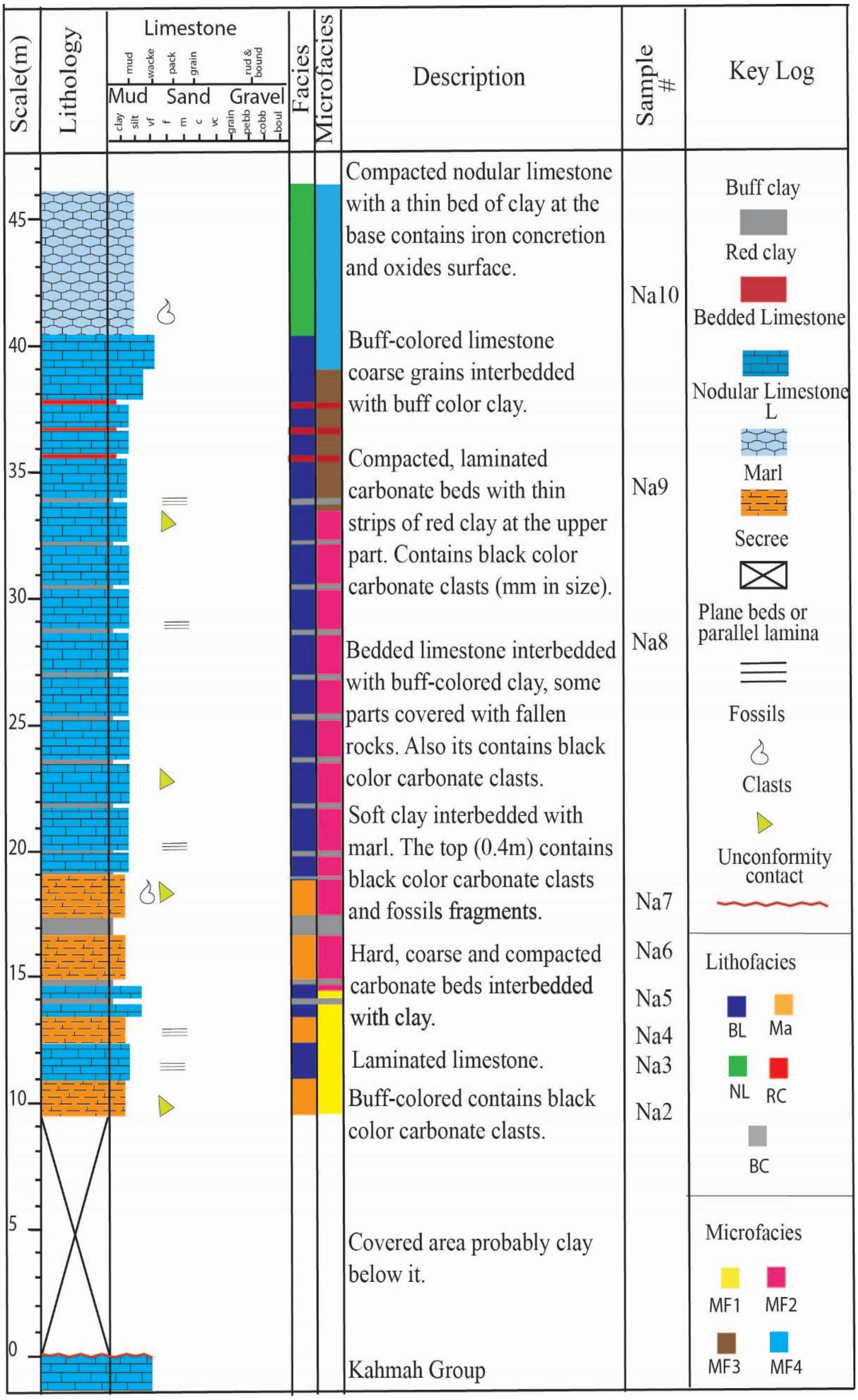

Figure 5. Sedimentological log of the Nakhal Section Na: (23° 23' 53.65" N; 57° 51' 1.25" E) showing the

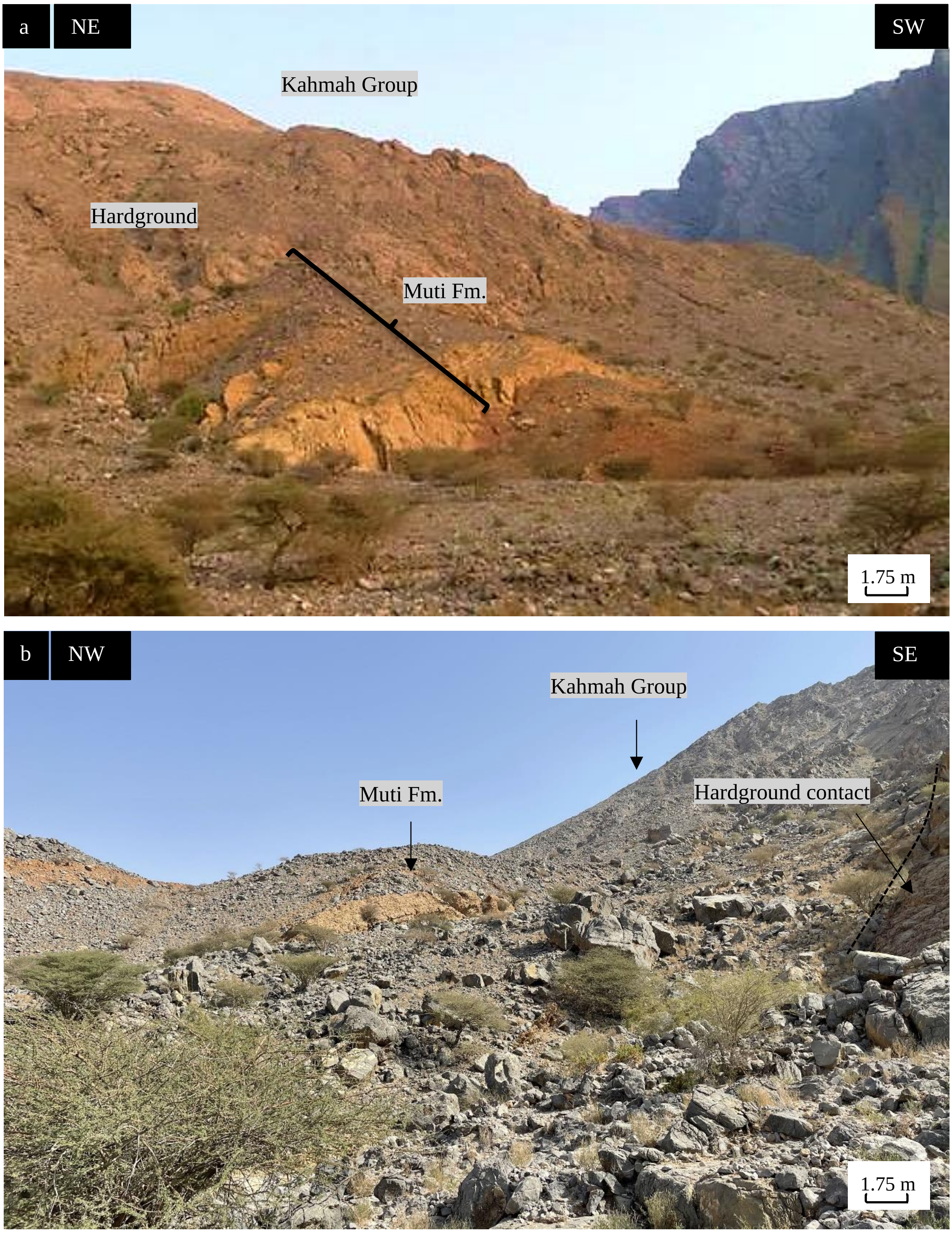

Figure 6. Field photographs of the studied sections in the Nakhal area showing the lower hardground contact between the Kahmah Group and the Muti Formation (A) Na section and (B) Nab section which consists of 10 to 12 meters of Nodular limestone.

Figure 7. Field photographs showing the lithofacies of the Muti Formation in Nakhal area section Na (a- e) section Nab (f); a- marl (Ma) contains black color carbonate clast (bcc), fossils fragments (ff), and red clay (rc); b- marl (Ma) contains angular to subangular white color carbonate clasts (wcc); c- red clay strips interbedded with bedded limestone; d- buff color clay interbedded with nodular limestone, e- nodular limestone lithofacies; f-nodular limestone in Nab section. Scale use: 50 Paisa Scale, lens 2.5 cm, hummer 32.5 cm, pen 13.5 cm, person around 1.75 m.

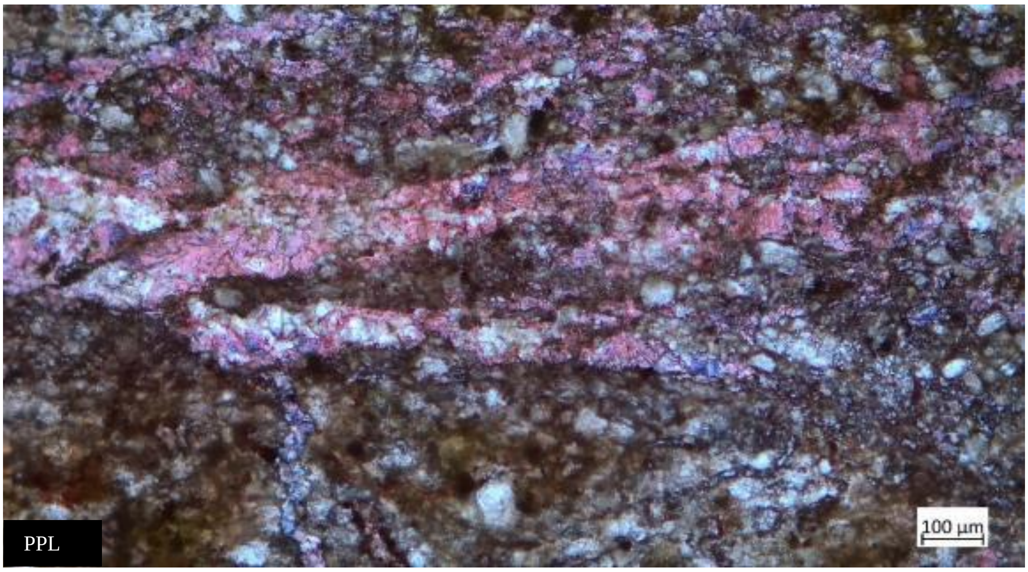

Figure 8. Microphotograph of thin section Na3 shows Alizarin Red S and Potassium Ferricyanide stain used for mineral identification. The calcite grains turn to red/pink color. The Fe-rich calcite distinguishes itself from the normal calcite by turning to blue color.

microfractures, which formed after the major fracture has been filled with cement, indicating two fracturing phases (Figure 9e). The carbonate cement that filled the fractures takes two forms: large calcite crystals (blocky) or sparry calcite cement (Figure 9 d, f). The blocky carbonate cement has subhedral to anhedral shapes and their sizes range from 50 µm to 450 µm. Part of the carbonate cement dissolved, creating a secondary porosity in one of the sparry calcite-filled fractures (Figure 9g). The porosity in the microfacies developed as non-fabric selective and is of two types: vuggy and channel (Figure 9h).

6.2.2. Microfacies 2: Bioclastic Packestone (MF2; SGP)

Bioclastic packstone microfacies is found in the middle of the Nakhal section, represented by three samples, Na8, Na7, and Na6 (Figure 10; Table 1). This microfacies is moderately to poorly sorted. In this microfacies, the carbonate mud matrix is mainly micrite (40%) and mixed with authigenic iron oxide patches (7%) represented by brown color. The remaining framework components are 35% non-skeletal grains and 19% skeletal grains.

The non-skeletal grains comprise 25% extraclasts grains of quartz, 8% iron oxide grains and around 1% peloids and micas, most likely, muscovite (Figures 10 a,b). The quartz grains are subangular to angular and medium to coarse silt-sized (Folk, 1959). They are distributed randomly within the microfacies. The peloid grains are ellipsoidal in shape, and their sizes range between 30 µm and 50 µm (Figures 10 a,b). The presence of mica suggests that they are derived from igneous and metamorphic rocks, particularly schists and phyllites [30].

The skeletal grains are preserved as outlined shapes of the complete fossils or parts of the fossils. The recognized fossils in this microfacies are bryozoan, planktonic foraminifera, calcisphere, bivalves, crinoids, and echinoid spines. The largest fossil fragment identified is a bryozoan (Figure 10c). The dimensions of this bryozoan fragment are around 3 cm in length and 0.5 cm in width. The bryozoans were also identified as small rectangular fragments measuring approximately 6 mm in length and 1.5 mm in width. Rare planktonic foraminifera of different types were detected. The planktonic foraminifera are filled with iron oxide, enveloped by iron or micrite. The types of foraminifera are uniserial foraminifera with seven champers (Ammobaculites sp.), multi-champer planisperial arranged in a helical coil (Falsotruncana sp.), biserial foraminifera (Planoheterohelix globulosa), rotaliid miliolida foraminifera (Nummofallotia cretacea), and Globigerinoides (Figure 10 d-g). A hollow spherical shape with a thin wall single layered of calcisphere is also present (Figure 10 h). Much of the single-layered Mesozoic calcispheres are cysts of planktonic algae [20]. Benthic foraminifera Laevidentalina sp. (Figure 10l), a calcispheres filled by micrite and enveloped by iron oxides, bivalves, dasycladacean algae, and crinoids are also observed in this microfacies (Figure 10i-k).

Diagenesis

Micritization and chemical compaction are the dominant diagenetic processes in microfacies 2. Micritization around the fossils is a most common diagenetic feature in this microfacies (Figure 10d). The micritization is created as a result of microscopic boring by algae or fungi. This suggests a low rate of sedimentation in the marine depositional system [30]. The chemical compaction is defined by stylolite, which is a zigzag linear feature of insoluble constituents such as clays or iron oxide minerals. Stylolites in this microfacies are present as sets of dissolution seams resulting in the stylo-laminated fabric (Figure 10m). This fabric develops when the amount of clay content is high, and the limestone is homogenous [20].

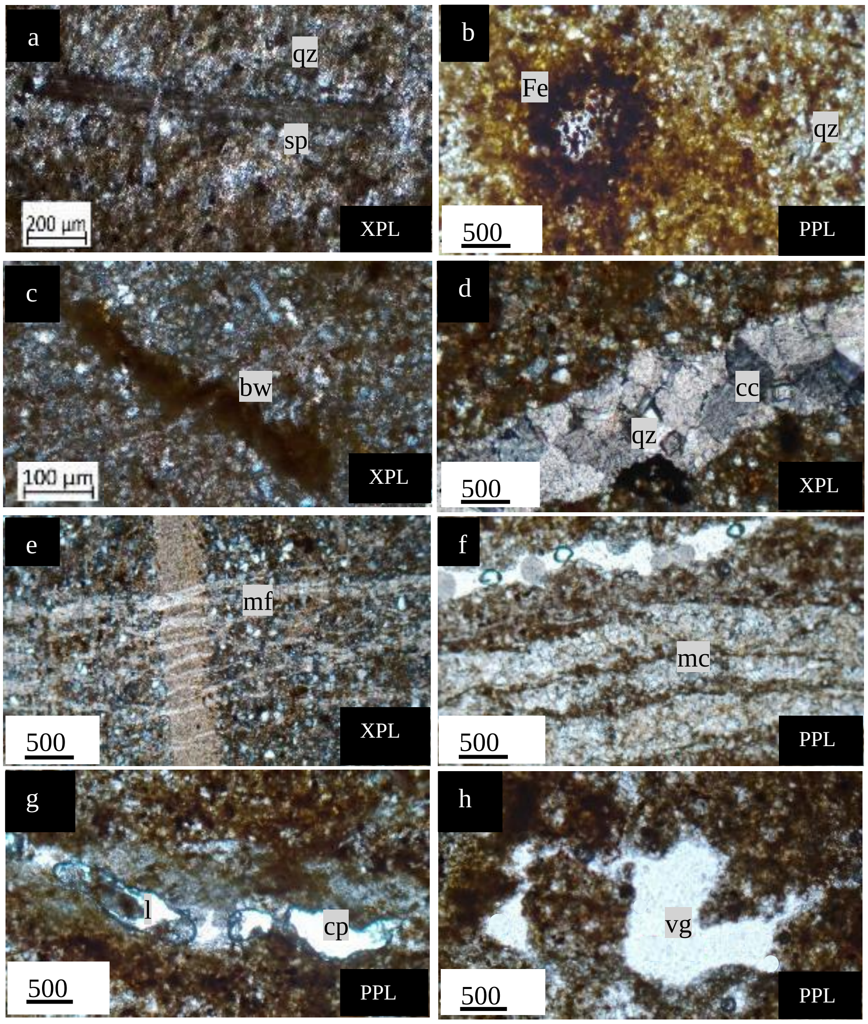

Figure 9. Microphotographs of echinoderm spines wackestone microfacies showing a- echinoderm spine (sp) and quartz grains in white/blue color (Qz), b- iron concretion yellow color (Fe) and quartz grains in white color (qz), c- burrows filled with iron (bw), d- fracture filled with blocky calcite cement (cc) and rare quartz grains (qz), e- microfractures (mf), f- sparry calcite cement filled fractures (mc), g- dissolutions of spar cement (l) and created secondary channel porosity (cp), and h- vuggy porosity (vg).

Furthermore, the presence of stylolite within the bryozoan fragment indicates the extent of chemical compaction (Figure 10c). The porosity observed in this microfacies is channel type (Figure 10n).

6.2.3. Microfacies 3: Arenaceous Wackestone (MF3; AW)

The arenaceous wackestone-dominated texture is represented by sample Na9 (Figure 11; Table 1). The microfacies is wackestone as the grain amount is more than 10% [18]. It is moderately to well sorted and randomly distributed. The framework components consist of micrite (65%), detrital quartz (20%), detrital iron oxide (5%), authigenic iron oxide (3%), zircon (in traces), skeletal grains (5%), and less than (1%) peloids.

The matrix is micritic and, in a few parts, rich with iron oxide (Figure 11a). The detrital quartz grains are distributed randomly within the microfacies. The quartz grains have low sphericity, subangular, and their sizes are coarse silt (0.03 mm to 0.06 mm) based on the Udden-Wentworth scale. The main bioclasts present are brachiopod fragments and planktonic foraminifera (Figures 11b-d). Different forms of iron oxides were identified, such as authigenic iron oxide nodules (3%) and detrital iron grains (5%) (Figure 11e).

However, the amount of bioclastic components, iron grains, and iron nodules in MF3 is much less compared with MF2.

Diagenesis

In this microfacies, diagenetic processes involve both fracture cementation and dissolution. These fractures, containing iron oxides and micrite, are distributed randomly. The dissolution of micritic cement selectively generates secondary porosity, as depicted in Figure 11f, and contributes to the development of non-fabric selective fracture porosity.

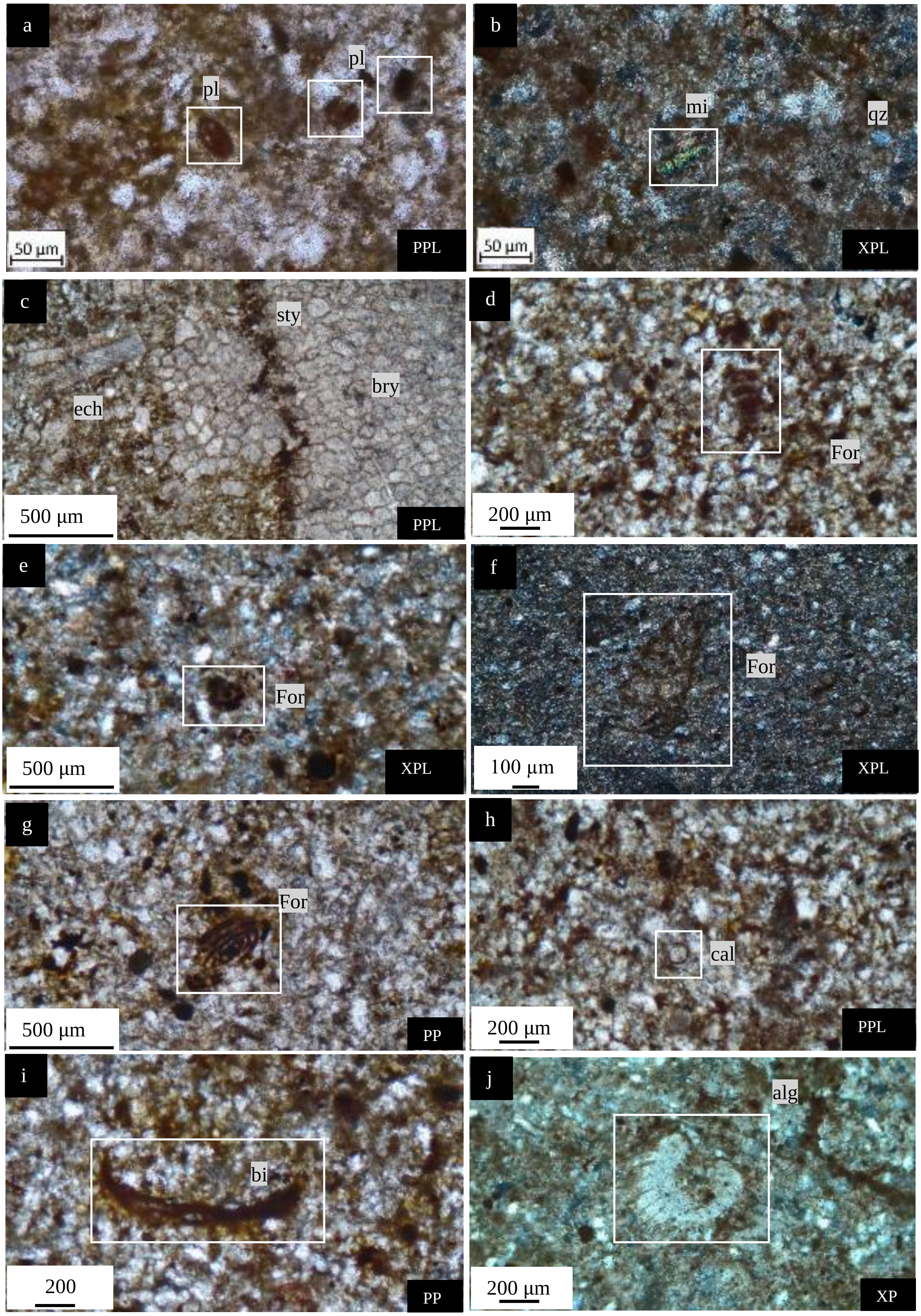
a
pl
pl
50 µm
PPL
b
mi
qz
50 µm
XPL
c
sty
bry
ech
500 µm
PPL
d
For
200 µm
e
For
500 µm
XPL
f
For
100 µm
XPL
g
For
500 µm
PP
h
cal
200 µm
PPL
i
bi
200
PP
j
alg
200 µm
XP

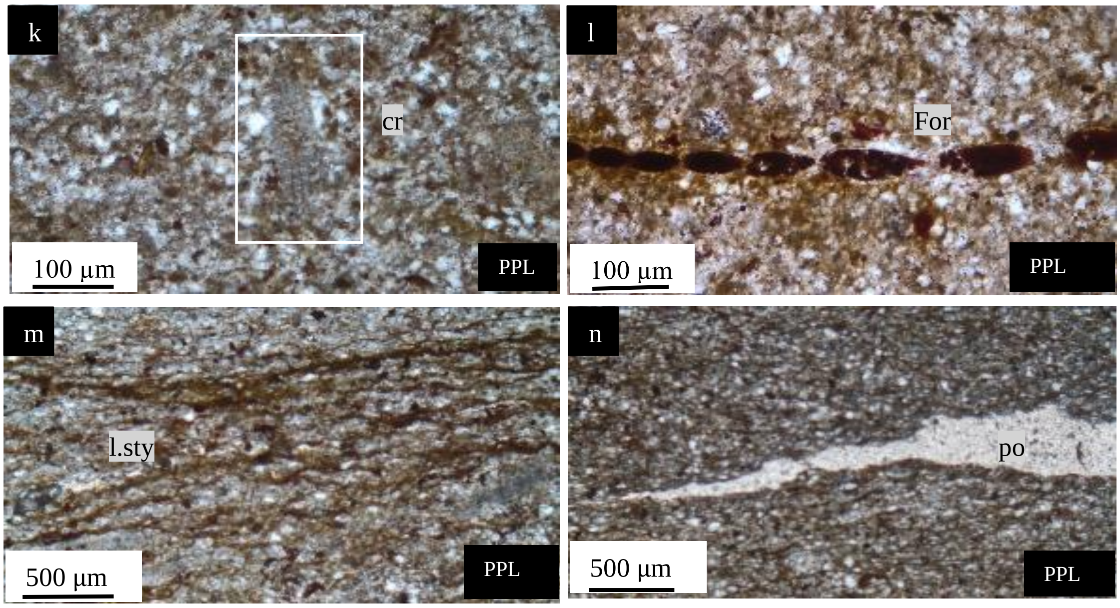

Figure 10. Microphotographs of skeletal grains packestone microfacies showing a- peloids (pl), b- mica (mi), c- bryozoan (bry) and echinoid fragments (ech) and stylolite (sty) within the bryozoan, d to g- foraminifera Ammobaculites sp., Falsotruncana sp., Planoheterohelix globulosa sp., Nummofallotia cretacea sp., h- calcisphere (cal), i- bivalves (bi), j- dasycladacean algae (alg), k-crinoids (cr), l- Benthic foraminifera Laevidentalina sp., m- stylo-laminated fabric (l.sty), and n- porosity (po).

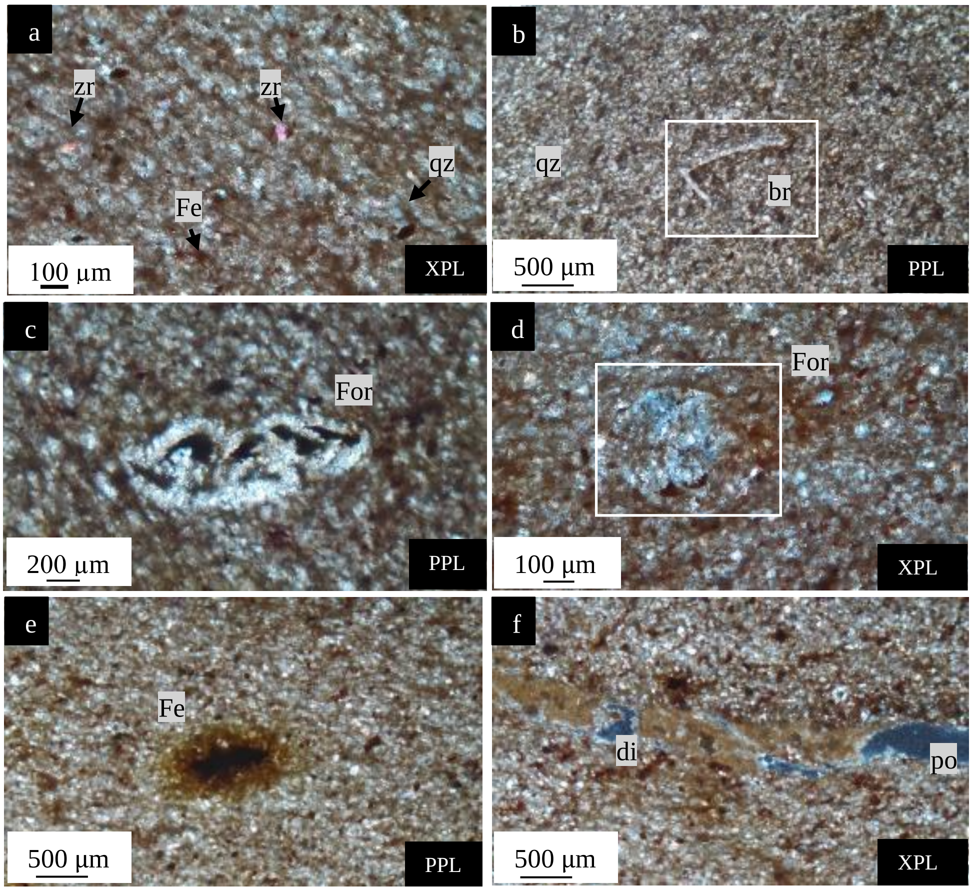

Figure 11. Microphotographs of arenaceous wackestone microfacies showing a- micritic mud and with iron oxides at places (Fe) and rare zircon (zr) and contains detrital quartz (qz), b- brachiopod fragment (br), c&d- planktonic foraminifera, e- iron nodule (Fe), and d- dissolution (di) and porosity (po).

6.2.4 Microfacies 4: Mudstone (MF4; MCM)

The mudstone microfacies belong to the grey-colored carbonate nodules of the nodular limestone lithofacies. It is classified based on Dunham's classification [18], indicating that the grains are less than 10%. The microfacies is homogenous (Figure 12 a). The matrix consists of microcrystalline calcite cement, constituting around 80% of the overall thin section composition (Figure 12)[26]. Detrital quartz constitutes around 5% of the total framework components of MF4. The quartz grains are subrounded, medium to coarse silt-sized quartz grains (Udden-Wentworth scale) (Figure 12a). The remaining framework components are distributed among peloids (3%), bioclasts (1%), traces of zircon and authigenic iron oxides (3%). Peloids are elongated to spherical in shape (Figure 12b). Moreover, minor amounts of microfossils were identified, such as calcispheres and undefined foraminifera fragments (Figure 12 a &c). The margins of the bioclasts are micritized, resulting in cortoids.

Diagenesis

The mudstone shows different diagenetic features, such as neomorphism, stylolite, fractures filled by cement, and micritization. The neomorphism is represented by recrystallization, which indicates the change in crystal sizes. The fractures are filled by either iron or calcite cement that appears coarser towards the center of the fracture (Figure 10d). The stylolite presents irregular lines of low amplitude peaks extending along the thin section (Figure 11e). Well-developed micritic envelopes surround the fossils (Figure 12c).

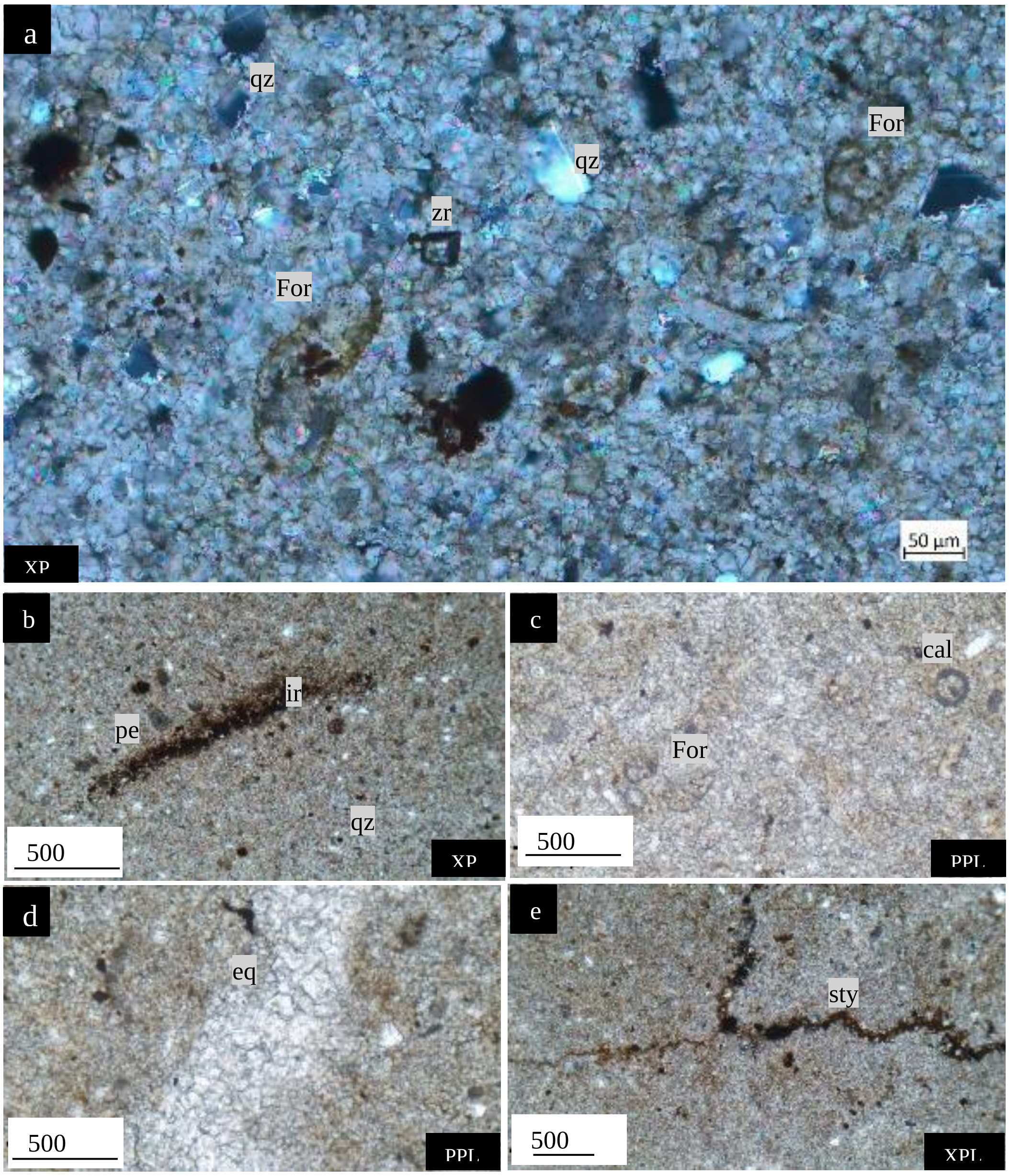

Figure 12. Microphotographs of mudstone microfacies show; a- microcrystalline cement, quartz (qz), and undefined foreminifera (For); b- peloids (pe), and burrow filled by iron (ir); c- calcisphere (cal) and foraminifera fragments (For); d- fracture filled by drusy equant calcite (eq), and; e- stylolite (sty).

7. Discussion

7.1 Diagenesis and Paragenetic Sequence

Diagenesis can be divided into three stages based on their timing and occurrence. These are known as eogenetic, mesogenetic, and telogenetic [32]. The eogenetic phase occurs near the seafloor, mesogenetic phase takes place during deep burial, and the telogenetic happens due to uplift and exposure to meteoric water conditions [15]. The diagenetic features observed within the studied formation are fractures, cementation, dissolution, stylolitization, micritization, and iron oxides. The paragenetic sequence of the Muti Formation in Nakhal Section Na is summarized in the following section (Figure 13).

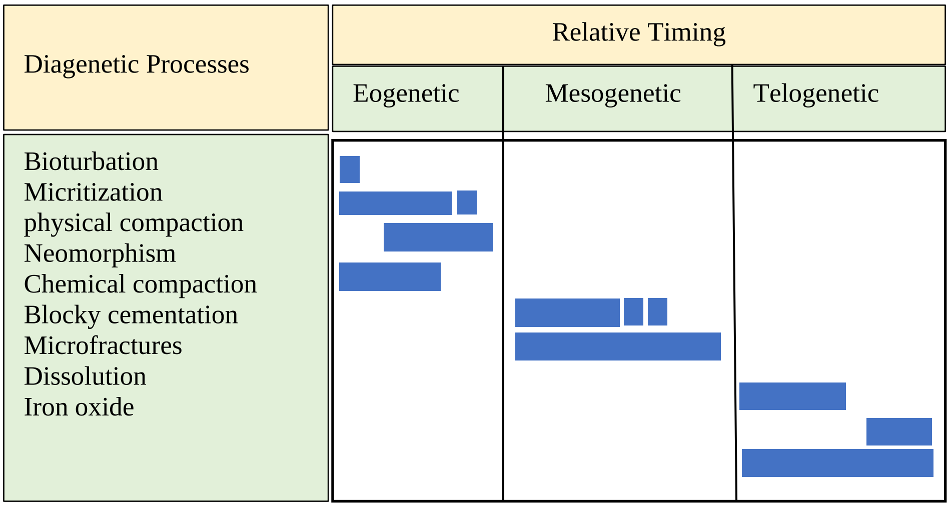

Figure 13. The paragenetic sequence of the main diagenetic features detected in the Muti Formation Nakhal section (Na). Note: small squares indicate not knowing the process's end time.

During the eodiagenensis stage, bioturbation, physical compaction, micritization, and neomorphism were the main processes. The bioturbation is characterized by the presence of burrows, indicating that burrowing took place on the sea floor before the sediment lithified, considered an early diagenetic process (Figures 9c &11b). Physical compaction, also referred to as mechanical compaction, begins immediately after the deposition due to the weight of the overlying sediments and is evidenced by the closely compacted framework components and point-to-point contact. Biogenetic activities, such as microborings by endolithic fungi and algae, can result in a thin coating of micrite around grains or bioclasts, forming a micrite envelope (Figures 10d, 12c) [15]. These processes occur in marine phreatic environments under low-energy subtidal settings [33]. The neomorphism in the Nakhal section is characterized as aggrading neomorphism, which involves an increase in the crystal size of carbonate minerals (Figure 12) [18, 32].

The burial environment, known as the mesogenetic stage, is subdivided into shallow and deep burials. The common diagenetic features observed during this stage are chemical compaction and cementation. Stylolites and dissolution seams are the main products of chemical compaction, and they are typically created at greater depths compared to physical compaction (Figure 10c, 10m). Stylolites are found within the micritic cement and bioclast. The pressure solution plays a significant role in providing a source of carbonate cement. The calcite cement is observed in the form of a blocky sparite and mosaic texture (Figures 9d, 12d).The telogenetic stage is related to the tectonic deformation during uplifted events. During this stage, the dissolution process occurs because of exposure to meteoric waters, resulting in formation of channels and vuggy porosity (Figures 9h, 11f). Also, diagenetic iron oxides and microfractures were created during the telogenetic stage (Figures 9b, 11e, 9e).

The characteristics of the nodular limestone observed in the studied area indicate that its formation can be attributed to in situ processes, such as differential compaction caused by thin clay interbeds within the limestone sequences. Moreover, diagenetic processes with varying sedimentation rates and compaction from one place to another may have contributed to the development of the nodules [26, 27].

7.2 Depositional Environment

The lithofacies within the Nakhal section vary from marl at the base to nodular limestone lithofacies at the top. The presence of marl lithofacies indicates deposition in quiet water setting, possibly in the back-shoal area. The marl lithofacies contain clay to silt size siliciclastic grains indicating transportation of fine sediments by currents under low energy conditions [21, 22]. On the other hand, the bedded limestone lithofacies were deposited under moderate energy settings in warm water conditions within the inner to outer shelf region [22]. The bioclastic packstone to wackestone microfacies in the bedded and nodular limestone indicate deposition in shallow subtidal zone, positioned below the fair-weather wave base but above the storm-wave base [23]. Clay-rich sediments, interbedded with limestone, were transported farther from their source areas and redeposited in middle shelf settings [23]. The outer shelf exhibits high diversity in terms of bioclasts.

The Mesozoic calcispheres are planktonic algae cysts, likely belonging to calcareous dinoflagellate, and have been observed to have a wide climatic range of distribution, commonly found in temperate regions [34]. They are typically deposited in quiet waters below the fair weather wave base. They are found in sedimentary environments ranging from the deeper shelf to slope and basinal settings, occasionally occurring in inner shelf environments [20]. In echinoderms, a phylum of marine organisms named Echinodermata, two members were recognized, echinoid and crinoids. Echinoids are commonly found in normal marine settings, such as open shelves or platforms [20]. On the other hand, crinoids were essential constituents of the open marine carbonate during the Mesozoic [35]. Planktonic foraminifera were one of the major marine planktonic constituent during the Cretaceous Period. Both smaller benthic and planktic foraminifera typically inhabit the open ocean under calm water conditions, mainly in the mid- to outer shelf areas. In addition, bryozoans were dominant organisms during the Late Cretaceous. They are predominated in the shelf sea and deposited in the middle to outer shelf regions. Bivalves, in general, are abundant in shallow marine settings, especially in shelf waters spanning from high- to low-latitude settings.

The microfacies within the studied formation exhibit a range of sediment compositions from mudstone to packstone based on Dunham classification [18]. Microfacies 1 corresponds to FZ 2 and SMF 9 of Flugel [15], which were deposited in the deep shelf settings (Figure 14). This microfacies is characterized by a micritic matrix, densely packed, and contains burrows and an abundance of echinoderms spines. It was deposited at low sedimentation rates, below fair-weather waves. Microfacies 2, associated with FZ3 and SMF 2, is situated at the toe of the slope (Figure 14). It consists of thin to medium-bedded limestone and is rich in bioclasts such as benthic foraminifera, crinoids and fragments of echinoid. Additionally, it contains peloids and fragments of extraclasts, such as quartz and mica. Microfacies 3 is related to FZ 2 and SMF 8, which were deposited in the outer shelf (Figure 14). The SMF 8 is characterized by the presence of sessile organisms, and in Microfacies 3, fragments of brachiopods and foraminifera were detected. This microfacies' deposition occurs in low-energy environments below the fair-weather wave base. Microfacies 4 corresponds to FZ 3 and SMF 3 and is deposited in the middle to outer shelf (Figure 14). It contains burrows and exhibits rare occurrences of fully micritized calcispheres and foraminifera dispersed in a micrite matrix. This microfacies was deposited under low energy conditions below the storm wave base. The litho- and microfacies of the Muti Formation in the studied section show detrital content in a major part of the formation. The Muti Formation in Nakhal Area was

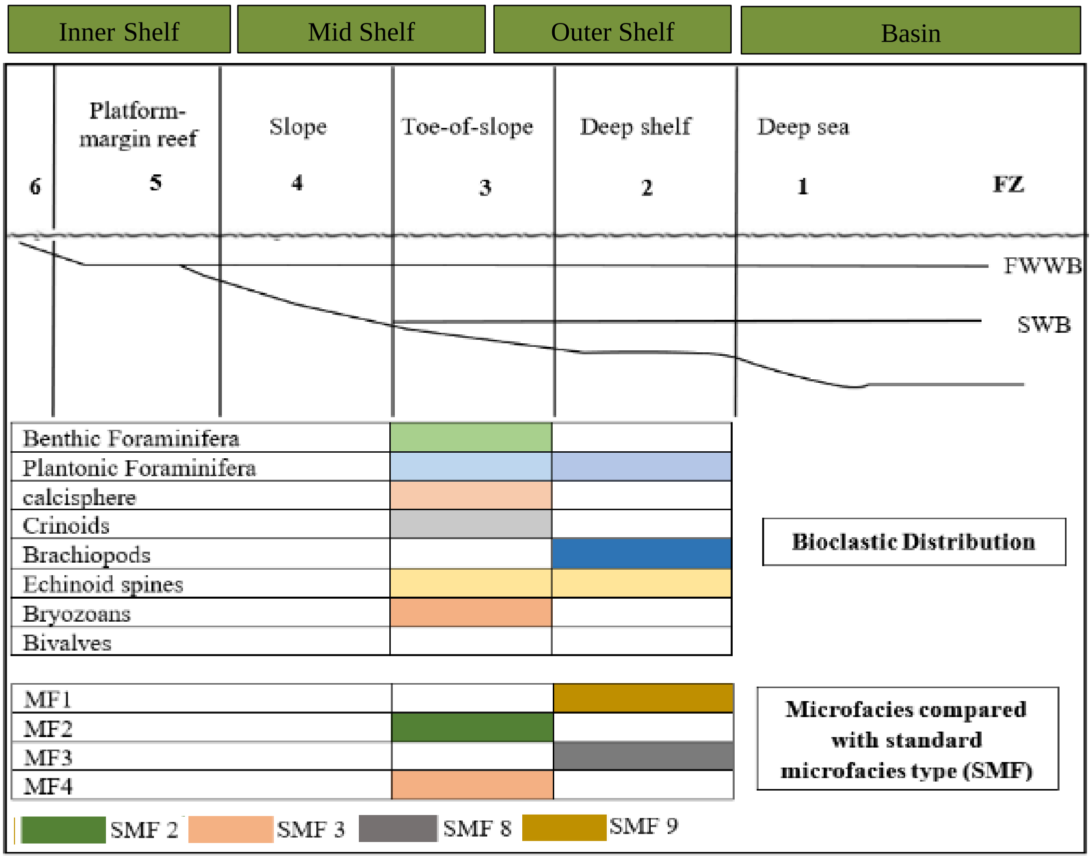

Figure 14. Depositional model of the Muti Formation showing the distribution of bioclasts and the studied microfacies compared with SMF based on Flugel, 2010; FZ facies zone. SMF 9 burrowed bioclastic wackestone; SMF 2 microbioclastic peloidal calcisiltite, SMF 8 wackestones and floatstones and SMF3 pelagic lime mudstone and wackestones.

deposited on top of the Kahmah Group, indicating erosion or non-deposition of the Wasia Group rocks from the area [15]. The top part of the Kahmah Group is represented by iron nodules possibly related to the platform drowing before the deposition of the Muti Formation. The marl lithofacies and Microfacies MF1 are common in the lower part of the formation indicating detritus input in the platform area. The Microfacies MF1 is rich in quartz content indicating detritus input from the cratonic area rather than the allochthonous units. The carbonate platform belonging to the Hajjar Supergroup gradually changed to a foreland basin [1] initially represented by the sediments of the Muti Formation in the study area. The lithofacies, microfacies and fossils content of the Muti Formation in the Nakhal area indicate that it was deposited in a shallow marine environment in the middle and outer carbonate shelves.

8. Conclusions

This study provides a comprehensive overview of the Muti Formation in the Nakhal area, revealing its thickness of about 50 m and consists of marl, bedded limestone, nodular limestone, and clay. Microfossil analysis identified various types, such as the bryozoan fragment, foraminifera, calcispheres, bivalves, fragments of echinoids, miliolida, and brachiopod fragments. Four distinct microfacies were identified: echinoderm spines wackestone, skeletal grains packestone, arenaceous wackestone, and mudstone. Lithofacies and petrographic analysis support the assumption that the Muti Formation in the Nakhal area was deposited in the middle and outer carbonate shelves during the Late Cretaceous. Micritization, burrowing, and mechanical compaction are common eodiagenetic alterations, whereas chemical compaction, physical compaction, cementation, and neomorphism are common mesodiagentic alterations. On the other hand, dissolution and secondary porosity creation are the dominant telodiagenetic alterations of the Muti Formation in the Nakhal section.

Conflict of Interest

The authors declare no conflict of interest.

Acknowledgment

This study was conducted through TRC grant RC/RG-SCI/ETHS/21/01. Special thanks to Dr. Mohammed Moustafa for preparing and helping in the Alizarin Red S and Potassium Ferricyanide stain processes. Many thanks to the Department of Earth Sciences lab technicians, including Hamdan Al Zidi, Bader Al Waili, Anas Al Rashdi, and Saeed Al Abri, for thin section preparation and lab assistance.

References

1. Robertson, A.H.F. Upper Cretaceous Muti Formation: transition of a Mesozoic nate platform to a foreland basin in the Oman Mountains. *Sedimentology*, 1987, **34(6)**, 1123-1142.
2. Warburton, J. Burnhill, T.J., Graham, R.H. and Isaac, K.P. The evolution of the Oman Mountains Foreland Basin. *Geological Society Special Publication*, 1990, **49**, 419-427.
3. Glennie K.W., Boeuf, M.G.A. Hughes Clarke, M.W. Moody-Stuart, M. Pilaar, W.F.H. and Reinhardt, B.M. Geology of the Oman Mountains (Parts 1, 2 and 3). The Hague, Martinus Nijhoff, Verhandelingen Koninklijk Nederlands Geologie en Mijnbouw Genootschap, 1974, **31**, 432.
4. Coleman, R.G. Tectonic setting for ophiolite obduction in Oman. *Journal of Geophysical Research*, 1981, 86(B4), 2497-2508.
5. Robertson, A.H.F. and Searle, M.P. The northern Oman Tethyan continental margin: Stratigraphy, structure, concepts and controversies. *Geological Society Special Publication*, 1990, **49**, 3-25.
6. Forbes, G.A., Janseni H.S.M., and Schreurs, J. Lexicon of oman subsurface stratigraphy, *Gulf PetroLink*, 2010, **15(3)**.
7. Ali, M.Y. Watts, A.B. and Searle, M.P. Seismic stratigraphy and subsidence history of the united arab emirates (UAE) rifted margin and overlying foreland basins. *Frontiers in Earth Sciences*, 2013, **5**, 17-44
8. Rabu, D., Bechennec, Beurrier and Hutin. Explanatory Notes of Nakhl Sheet NF 40-3E, Scale 1:100000. B.R.G.M. *Ministry of Petroleum and Minerals*, 1986.
9. Loosveld, R.J.H. Bell, A. and Terken, J.J.M. The tectonic evolution of interior Oman. *GeoArabia*, 1996, **1(1)**, 28-51.
10. Ali, M.Y. and Watts, A. B. Subsidence history, gravity anomalies and flexure of the United Arab Emirates (UAE) foreland basin. *GeoArabia*, 2009, **14(2)**, 17-44.
11. Jolivet. L. Neo-tethys geodynamics and mantle convection: From extension to compression in Africa and a conceptual model for obduction. *Canadian Journal of Earth Sciences*, 2016, **53(11)**, 1190-1204.
12. Boote, D.R.D, Mou, D and Waite, R.I. Structural evolution of the Suneinah Foreland, Central Oman Mountains. *Geological Society Special Publication*, 1990, **49**, 397-418.
13. Glennie, K.W. Hughes Clarke, M.W. Boeuf, M.G.A. Pilaar, W.F.H. and Reinhardt, B.M. Inter-relationship of Makran-Oman Mountains belts of convergence. *Geological Society Special Publication*, 1990, **49**, 773-786.
14. Mattern, F., Pracejus, B., Scharf, A., Frijia, G., Al-Salmani, M. Microfacies and composition of ferruginous beds at the platform-foreland basin transition (Late Albian to Turonian Natih Formation, Oman Mountains): Forebulge dynamics and regional to global tectono-geochemical framework, *Sedimentary Geology*, 2022, **429**, 106074.
15. Rabu, D., Bechennec, Beurrier and Hutin. Explanatory Notes of Nakhl Sheet NF 40-3E, Scale 1:100000. B.R.G.M. *Ministry of Petroleum and Minerals*, 1986.
16. Stern, R.J. and Johnson, P. Continental lithosphere of the Arabian Plate: A geologic, petrologic, and geophysical synthesis. *Earth-Science Reviews*, 2010, **101(1-2)**, 29-67.
17. Dickson, J.A.D. A Modified staining technique for carbonates in thin section, *Nature*, 1965, **205(7)**.

18. Robert. J. Dunham. Classification of Carbonate Rocks According to Depositional Textures, in Classification of Carbonate Rocks-A Symposium, *William E. Ham*, 1962.
19. Searle, M.P. Structural geometry, style and timing of deformation in the Hawasina Window, Al Jabal al Akhdar and Saih Hatat culminations, Oman Mountains. *GeoArabia*, 2007, **12(2)**, 99-130.
20. Flügel, E. Microfacies of Carbonate Rocks, *Springer Science and Business Media*, 2010.
21. Nichols, G. Sedimentology and Stratigraphy. *John Wiley and Sons.* 2nd Edition. 2009.
22. James, N.P. and Walker, R.G. Facies Models: response to sea level changes. *Geological Association of Canada*, 1992.
23. Scholle, P.A. Bebout, D.G. and Moore, C.H. Carbonate Depositional Environments. *AAPG Memoir*. 1983.
24. Woo, J. Lee, H. Ozyer, S.C. and Rhee, C.W. Effect of Lamination on Shale Reservoir Properties: Case Study of the Montney Formation. Canada. *Geofluids*, 2021, vol. 2021.
25. Scott, R.W. Chronostratigraphy of the Cretaceous carbonate shelf, southeastern Arabia. *Geological Society Special Publication*, 1990, **49**, 89-108.
26. Banerjee, S. Jeevankumar, S. Sanyal, P. and Bhattacharyya, S.K. Stable isotope ratios and nodular limestone of the Proterozoic Rohtas limestone. Vindhyan basin, India. *Carbonates Evaporites*, 2006, **21(2)**, 133-143.
27. Bjørlykke, K. Sediment Compaction and Rock Properties. *AAPG International Conference and Exhibition*. 2009.
28. Scholle, P.A. A Colour Guide to Carbonates: Carbonate Rock Constituents, Textures, Cements, and Porosities. *AAPG Memoir*, **27**, 1978.
29. Terry, R.D. and Chilingar, G.V. Summary of Concerning some additional aids in studying sedimentary formations, by M.S. Shvetsov. *Journal of Sedimentary Research*, 1955, **25(3)**.
30. Tiwari, R.N. Experiment-8 Microscopic Study of Common Sedimentary Rocks. *Indira Gandhi National Open University*, New Delhi, 2020.
31. Scholle, P.A. and Ulmer-Scholle, D.S. A colour guide to the petrography of carbonate rocks: Grains, textures, porosity, diagenesis, *AAPG Memoir*, 2005, **77**.
32. Scholle, P.A. 1978. A Colour Illustrated Guide to Carbonate Rock Constituents, Textures, Cements, and Porosities. *AAGP Memoir*, Tulsa, Oklahoma, 1978, **115(6)**, 473.
33. Boggs, S. Principles of stratigraphy and sedimentology. Principles of stratigraphy and sedimentology, *Pearson*, 2006.
34. Berkyová, S. and Munnecke, A. Calcispheres' as a source of lime mud and peloids evidence from the early Middle Devonian of the Prague Basin, the Czech Republic. *Bulletin of Geosciences*, 2010, **85(4)**, 585-602.
35. Scholle, P.A. and Ulmer-Scholle, D.S. A Colour Guide to the Petrography of Carbonate Rocks, AAPG, 2020.